European Journal of Taxonomy 930: 182–204
https://doi.org/10.5852/ejt.2024.930.2493
ISSN 2118-9773
www.europeanjournaloftaxonomy.eu
2024 · Sánchez-Ruiz A. & Bonaldo A.B.

Research article

urn:lsid:zoobank.org:pub:A749FA5A-AFCF-4C58-AA43-6953B5693462

Updating the morphological phylogenetics of Nopinae (Araneae: Caponiidae): novel terminals and characters, with two new species

Alexander SÁNCHEZ-RUIZ [1,*] & Alexandre B. BONALDO [2]

[1,2] Museu Paraense Emílio Goeldi, Coordenação de Zoologia, Laboratório de Aracnologia, Av. Perimetral, 1901, Terra Firme, CEP 66077−830, Belém, Pará, Brazil.

[*] Corresponding author: alex.sanchezruiz@hotmail.com
[2] Email: bonaldo@museu-goeldi.br

[1] urn:lsid:zoobank.org:author:D312037D-5F2B-4F86-A822-F0BAD1BEF20A
[2] urn:lsid:zoobank.org:author:118CFCBA-BD7E-4F15-8412-4979159298BA

Abstract. A re-analysis of the morphological phylogeny of the Nopinae is made, based on an update in the description of *Aamunops* Galán-Sánchez & Álvarez-Padilla, 2022 and the addition of the recently described genera *Nopsma* Sánchez-Ruiz, Brescovit & Bonaldo, 2020 and *Roddemberryus* Sánchez-Ruiz & Bonaldo, 2023. Two new species, *Aamunops hoof* sp. nov. (male) and *Aamunops yiselae* sp. nov. (male and female), are also described, which allows a better understanding of the genus morphology and resulted in an emended diagnosis. The description of *Aamunops* has been updated to include several characteristics of the ultrastructural morphology, legs, chelicerae, palps and female genitalia. The inclusion of these new characters of *Aamunops* along with those of *Nopsma* and *Roddemberryus* in the previous data matrix resulted in a new, completely different hypothesis of the relationships of the nopine genera: *Nopsma* is part of a group formed by *Cubanops* and *Nyetnops*, while *Aamunops* and *Roddemberryus* are grouped with representatives of *Tarsonops*. The four-eyed *Nopsides ceralbonus* Chamberlin, 1924 was recovered as the most basal species of Nopinae. The relationships among genera of Nopinae and the phylogenetic position of three species, whose taxonomic position is doubtful (*Cubanops luquillo* Sánchez-Ruiz, Brescovit & Alayón, 2015, *Orthonops confuso* Galán-Sánchez & Álvarez-Padilla, 2022 and *Tarsonops irataylori* Bond & Taylor, 2013), is also discussed.

Keywords. Synspermiata, nopines, taxonomy, Neotropical region.

Sánchez-Ruiz A. & Bonaldo A.B. 2024. Updating the morphological phylogenetics of Nopinae (Araneae: Caponiidae): novel terminals and characters, with two new species. *European Journal of Taxonomy* 930: 182–204. https://doi.org/10.5852/ejt.2024.930.2493

Introduction

The morphology of spiders of Caponiidae Simon, 1890 has been studied in recent years, mainly thanks to the works of Sánchez-Ruiz *et al.* (2015), Brescovit & Sánchez-Ruiz (2016) and Sánchez-Ruiz & Brescovit (2017, 2018), where, in addition to the taxonomy, topics of the morphology and nomenclature of some of

the structures have been covered. These spiders are morphologically unusual in several characteristics of the legs, endites, carapace and eyes. The legs of Nopinae Petrunkevitch, 1939 exhibit modifications such as adesmatic joints and bizarre membranous modifications (crista, gladius and arolium) on the distal leg podomeres (Sánchez-Ruiz & Brescovit 2017). Nopines are also notorious for the reduction in the number of eyes: with the exception of one species, *Nopsides ceralbonus* Chamberlin, 1924 with four eyes, all other nopines are two-eyed species. On the other hand, some non-nopine genera have a highly modified carapace and endites (Brescovit & Sánchez-Ruiz 2016); and the number of eyes varies greatly among genera, ranging from eight-, six-, four- and two-eyed species to completely blind caponiids.

In addition to the presence, size, and shape of the three membranous structures of the nopine legs, the presence and number of adesmatic joints present in the tarsi and metatarsi are also informative. These false sutures are found only in the nopine genera and are present in two different forms: single and multiple adesmatic joints. All nopines have at least a single adesmatic joint on the tarsi. In fact, the presence of this false tarsal suture is considered a synapomorphy for the subfamily (Sánchez-Ruiz & Brescovit 2018; Galán-Sánchez & Álvarez-Padilla 2022). Some genera such as *Cubanops* Sánchez-Ruiz, Platnick & Dupérré, 2010, *Roddemberryus* Sánchez-Ruiz & Bonaldo, 2023 and *Tarsonops* Chamberlin, 1924 also have adesmatic joints in the metatarsi (Sánchez-Ruiz *et al.*2010; Sánchez-Ruiz & Brescovit 2015; Sánchez-Ruiz & Bonaldo 2023). The number and distribution of adesmatic joints on the legs vary in these genera. While *Cubanops* presents a wide, single metatarsal adesmatic joint only in the metatarsus IV, *Tarsonops* and *Roddemberryus* present multiple metatarsal adesmatic joints in all metatarsi, intertwined on the cuticle, with specific limits poorly defined, causing the leg to even bend in that segment.

The phylogenetic structure of Nopinae was first addressed by Sánchez-Ruiz & Brescovit (2018), with a data matrix composed of 41 terminal species (most of which were *Nops* MacLeay, 1839), representing nine genera. Galán-Sánchez & Álvarez-Padilla (2022) proposed *Aamunops* Galán-Sánchez & Álvarez-Padilla, 2022, and tested its phylogenetic position among nopines using that data matrix. Studying caponiid specimens from Mexico, we found two new species of *Aamunops* which are described below. This discovery allowed us to update the diagnosis and description of *Aamunops* to include several characteristics of the leg and chelicerae ultrastructural morphology such as tarsal organ, trichobothria, slit sensillae and pretarsal setae, as well as new information on legs, chelicerae, endites, palps and female genitalia. We found that these two new species and their known congeners show a few, wide adesmatic joints restricted to a small portion of the apical third of metatarsus IV, similar to those present in the metatarsi IV of *Cubanops*. Here, we re-access the phylogeny of Nopinae, adding new morphological information on *Aamunops* and on the recently described genera *Roddemberryus* and *Nopsma* Sánchez-Ruiz, Brescovit & Bonaldo, 2020, to the data matrix presented by Sánchez-Ruiz & Brescovit (2018), proposing an updated hypothesis of the relationships among these lineages.

Material and methods

Repositories

The specimens examined were supplied by the following collections (curators between parentheses):

AMNH = American Museum of Natural History, USA (L. Prendini)
BSC = Centro Oriental de Ecosistemas y Biodiversidad, Cuba (C. Plasencia)
CARCIB = Centro de Investigaciones Biológicas del Noroeste, Mexico (M.L. Jiménez)
CAS = California Academy of Sciences, USA (L. Esposito)
CNAN = Colección Nacional de Arácnidos, Instituto de Biología, Universidad Nacional Autónoma de México, México (E. González-Santillán)
IAvH-I = Instituto Alexander Von Humboldt, Bogotá, Colombia (J.C. Neita)
IBSP = Instituto Butantan, Brazil (A.D. Brescovit)
INBIO = Instituto Nacional de Biodiversidad, Costa Rica (C. Víquez)

MCTP = Museu de Ciências e Tecnologia, Pontifícia Universidade Católica do Rio Grande do Sul, Brazil (R. Teixeira)
MCZ = Museum of Comparative Zoology, USA (G. Giribet)
MNHNCu = Museo Nacional de Historia Natural, Cuba (G. Alayón)
NCA = National Collection of Arachnida, Queenswood, South Africa (P. Marais)
NHM = Wiener Naturhistorischen Museum, Austria (C. Hörweg)
QCAZ = Museo de Zoología, Pontificia Universidad Católica de Quito, Equador (A. Barragán)

Characters and terminals

Several new additions and emendations were made to the set of characters published by Sánchez-Ruiz & Brescovit (2018), based on the study of new material and the addition of 12 species to the proposed matrix (see Supp. file 1). The characters added by Galán-Sánchez & Álvarez-Padilla (2022) were reinterpreted in the light of the new morphological characteristics found in *Aamunops*. A total of 54 characters were studied, of which 17 were reinterpreted and six were newly added. Characters 7, 20, 29, 39, 42 and 46 are uninformative in the present dataset but were left in the matrix with the intention of allowing the integration of the present dataset into more comprehensive studies. The dataset includes 25 species representing all 10 known genera of Nopinae (see Supp. file 2) and two genera of non-Nopinae as outgroups. We kept all terminals studied by Sánchez-Ruiz & Brescovit (2018), except in the case of *Nops*, of which we included only three species representing the main Neotropical areas: the Caribbean *Nops guanabacoae* MacLeay, 1839 (type species), the Central American *Nops largus* Chickering, 1967 and the South American *Nops meridionalis* Keyserling, 1891. Two or three representative species of each genus of Nopinae were added (the type species of each genus, plus one or two species belonging to different morphological groups within each genus). Three species with doubtful taxonomic position were also added (*Cubanops luquillo* Sánchez-Ruiz, Brescovit & Alayón, 2015, *Orthonops confuso* Galán-Sánchez & Álvarez-Padilla, 2022 and *Tarsonops irataylori* Bond & Taylor, 2013). These are the only terminals for which only males are known. All other species are represented by both sexes in the data matrix. Representatives of *Nopsma*, *Roddemberryus* and the new species *Aamunops yiselae* sp. nov. were studied and scored for the first time in this work. The other representative of *Aamunops* (*A. olmeca* Galán-Sánchez & Álvarez-Padilla, 2022) and *Orthonops confuso*, also added to this updated dataset, were scored based on the description of Galán-Sánchez & Álvarez-Padilla (2022).

Phylogenetic analysis

The updated dataset for cladistic analysis comprises 53 characters (Supp. file 3) and 25 terminal taxa (Supp. file 2). Multistate characters were treated as non-additive. The dataset and trees were manipulated using the program WinClada 1.00.08 (Nixon 2002). The parsimony analyses were performed in TNT 1.1 (Goloboff *et al.* 2008) using the New Technology Search with the algorithms 'tree fusing', 'ratchet' and 'sectorial searches', and with the same command lines as in Sanchez-Ruiz & Brescovit (2018) (command: *hold 20000; xmult = hits 15 ratchet 10; bb = fillonly;*). Clade support was estimated through Jackknifing with a 36% change probability and 1000 replicates (command: *mult:noratchet repl 100 tbr hold 10; resample jak repl 1000 freq from 0 [mult];*), and by Bremer support values (command: *hold 10000; sub 20; bb = fillonly tbr; bsupport;*).

Morphological methods

Morphological observations were made using a Leica MZ12 stereo microscope. Coloration patterns are described based on specimens preserved in 80% ethanol. Internal female genitalia were dissected, and soft tissues were digested for 24 hours with Ultrazyme® enzymatic eye lens cleaner, diluted with distilled water at the proportion of 1 tablet / 5 ml. Descriptions and terminology for copulatory structures mostly follow Sánchez-Ruiz *et al.* (2015) and Sánchez-Ruiz & Brescovit (2018). The updated morphological description of *Aamunops* includes solely the new additions and emendations made to the original description; other

characteristics from the original description were only corroborated in the new species described here. Measurements are in millimetres (mm) and were made using a microscope micrometer eyepiece. Digital SEM micrographs were taken using a TESCAN Mira3 scanning electron microscope at the Museu Paraense Emilio Goeldi, following standard procedures for sample preparation. Multifocal photos were taken with a Leica MC170 HD digital camera attached to a Leica M205 C stereo microscope, using Leica Application Suite ver. 4.10 software. Distribution maps were generated with ArcView® ver. 9.0 and edited with Adobe Photoshop CC 2015 ver. 5.1. All figures in the paper were edited using Adobe Photoshop® CC 2015 ver. 5.1.

Abbreviations

Ac	=	aciniform gland spigot
aj	=	adesmatic joints
ALS	=	anterior lateral spinnerets
amr	=	anteromendian receptacle
ap	=	posterior plate
arb	=	anteromendian receptacle base
ca	=	crista
cml	=	cheliceral membranous lobes
CS	=	cheliceral slit sensilla
ess	=	external sclerotization around spiracles
eo	=	embolar opening
gl	=	gladius
go	=	genital opening
hp	=	hyaline process
IC	=	pretarsal unpaired claw
ip	=	posterior invagination
MaAm	=	major ampullate gland spigot
MiAm	=	minor ampullate gland spigot
mp	=	median projection
MtS	=	dorsal metatarsal stopper
pfs	=	patch of frictional setae on ventral-apical part of tarsi
Pi	=	piriform gland spigot
PLS	=	posterior lateral spinnerets
PMS	=	posterior median spinnerets
pp	=	posterior plate
pr	=	posterior receptacle or interpulmonary fold
pRS	=	promarginal rake setae on chelicera
psb	=	pair of sclerotized bars (transverse rigid plate)
rRS	=	retromarginal rake setae on chelicera
sac	=	membranous sac-like structure
t	=	tracheal trunk

Results

Phylogenetics

The cladistic analysis under equal weights resulted in two most parsimonious trees of 98 steps, consistency index Ci = 0.68 and retention index Ri = 0.85 (deactivating six uninformative characters). The strict consensus of these two trees is shown in Fig. 1. We also analyzed the data matrix under implied weighting, with constants of concavity k = 1 to 12. Under k = 1, seven trees were obtained, differing one from each other mainly in the position of the species of *Orthonops* Chamberlin, 1924, *Medionops* Sánchez-Ruiz &

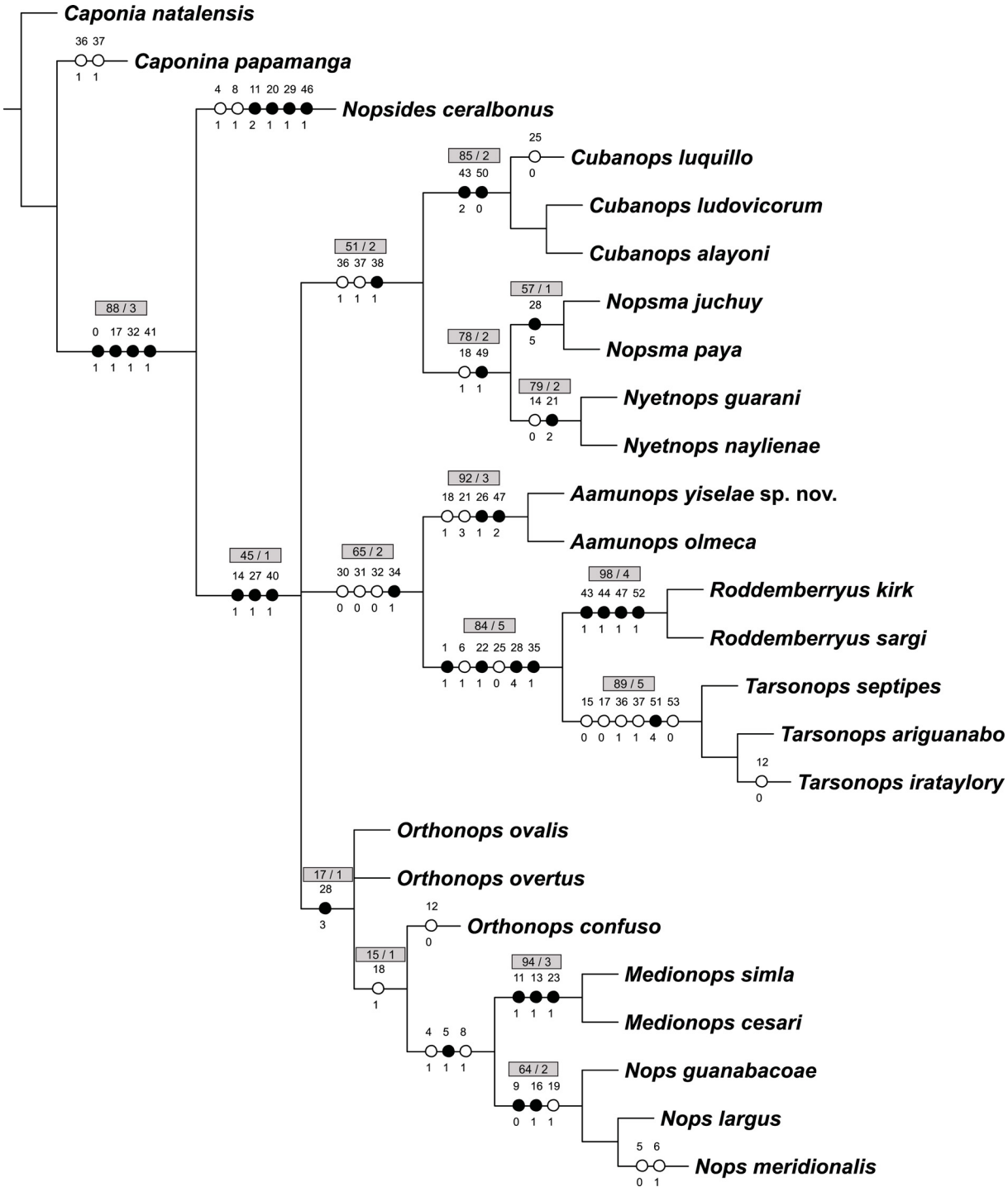

Fig. 1. Consensus tree using equal character weights (L = 98, Ci = 0.68, Ri = 0.85). Filled and open circles represent non-homoplasious and homoplasious transformations, respectively. Only synapomorphies common to both cladograms were included. Character numbers are placed over the branches and the states are shown below the branches. Numbers above branches with colored background are Jackknife percentages (left) and Bremer support values in units of fit (right).

Brescovit, 2017 and *Nops*. Under k = 2, the same two trees were obtained as were obtained under the equal weights. On the other hand, under concavities 3–12, a single tree was obtained. The most striking difference between this tree and the tree obtained under the equal weighting is the depiction of a large clade composed of the species of *Aamunops*, *Roddemberryus*, *Tarsonops*, *Orthonops*, *Medionops* and *Nops*, which was not retrieved by the equal weight consensus in Fig. 1. Since the support for this clade of six genera is low, we chose to limit the discussion below to the topology obtained under equal weighting.

Monophyly of Nopinae

The updated hypothesis recovered the monophyly of Nopinae with high support values: jackknifing = 88%; Bremer support BS = 3 (Fig. 1). Members of Nopinae are supported by four unambiguous synapomorphies. However, two of these synapomorphies (characters 32[1], 41[1]) could become homoplastic when non-nopine genera are added to the dataset. Nopines are a monophyletic group by the presence of the tarsal adesmatic joints (0[1]) and the presence of a dorsal chemosensory patch on the palps (17[1]). Similar results were also obtained by Sánchez-Ruiz & Brescovit (2018) and Galán-Sánchez & Álvarez-Padilla (2022). All nopines have the tarsal adesmatic joints in all legs, and although most nopines have only one adesmatic joint in the tarsi, at least two genera (*Tarsonops* and *Roddemberryus*) have multiple false sutures in both the tarsi and metatarsi. On the other hand, the palpal dorsal chemosensory patch is present in almost all nopines, except for *Tarsonops*, an absence here interpreted as secondary.

Updated topology

With the inclusion of the members of *Nopsma*, *Aamunops* and *Roddemberryus* in our dataset, the topology obtained by Sánchez-Ruiz & Brescovit (2018) and Galán-Sánchez & Álvarez-Padilla (2022) was completely modified (Fig. 1). *Nopsma* is part of a group formed by *Cubanops* and *Nyetnops*, characterized by the presence of a cephalotoracic pattern (38[1]). *Aamunops* and *Roddemberryus* make a group with representatives of *Tarsonops*, characterized by including only the nopines with a partially membranous and horizontal interpulmonary fold (34[1]) and a narrow and long anteromendian receptacle (30[0]).

Taxonomy

Class Arachnida Cuvier, 1812
Order Araneae Clerck, 1757
Family Caponiidae Simon, 1890
Subfamily Nopinae Petrunkevitch, 1939

Genus ***Aamunops*** Galán-Sánchez & Álvarez-Padilla, 2022

Type species

Aamunops olmeca Galán-Sánchez & Álvarez-Padilla, 2022 by original designation.

Emended diagnosis

Members of *Aamunops* can be distinguished from all non-nopines genera by the presence of adesmatic joints on the tarsi (Figs 2H, 3G, 4H–I); males differ from all other Nopinae by the presence of a hyaline process associated with the seminal duct, protruding near the embolus tip (Fig. 5A–B), and females by the presence of a sclerotized-bifid duct on the anteromedian receptacle base (Fig. 6D).

Other species included

A. chimpa Galán-Sánchez & Álvarez-Padilla, 2022, *A. hoof* sp. nov., *A. misi* Galán-Sánchez & Álvarez-Padilla, 2022, *A. noono* Galán-Sánchez & Álvarez-Padilla, 2022 and *A. yiselae* sp. nov.

Description

Described by Galán-Sánchez & Álvarez-Padilla (2022: 55). New data and emendations: anterior median eyes dark, situated on slightly elevated black tubercle (Figs 2C, 3C, 4C). Chelicerae with promarginal and retromarginal rake setae on the anterior and posterior margins of the fang furrow (Fig. 7D–F), even reaching ectal side; a few retromarginal slit sensilla on the apical side of chelicerae (Fig. 7E). Endites with a short posterior basal projection, more pronounced in males (Figs 2G, 3D, 4D). Legs without spines; coxae I–II also with a short posterior basal projection, coxae III–IV without basal projections (Figs 2G, 3D, 4D); anterior femora enlarged, three times (or less) as long as wide (Fig. 8A–B); metatarsi I, II and III entire, metatarsus IV with a few, wide adesmatic joints restricted to a small portion in the apical third of metatarsus (Figs 2H, 3G, 4H–I, 9E–F); gladius enlarged, short, sword-shaped (Fig. 8C–E), the most common shape among nopines; all tarsi bi-segmented with a single adesmatic joint (Fig. 8E), pretarsus without a perceptible arolium (Figs 10A, 11B), unpaired claws short on all legs, smooth without small teeth (Figs 10A, 11A); few ventral frictional setae on tarsi and several other setae around pretarsal claws (Fig. 10A–B, F); tibiae, metatarsi, and tarsi with trichobothria in a single row, bases with semicircular rim bearing slight longitudinal ridges (Fig. 10C–D), tarsal organ exposed, roundish, with marginal ring slightly pronounced (Figs 10E, 11D), slit sensilla on tibiae, metatarsi and tarsi (Fig. 11C). Female spinnerets with one major ampullate gland and two piriform gland spigots on ALS (Fig. 12A, C), one presumed minor ampullate gland and an aciniform gland spigots field with at least up to nine glands on PMS (Fig. 12C), at least eleven aciniform gland spigots on PLS (Fig. 12D). Female palpal femur arcuate upwards (Fig. 4E–F), male palpal femur straight (Fig. 2D–E). Male embolus long in *A. chimpa*, *A. misi* and *A. olmeca*, short in *A. hoof* sp. nov., *A. noono* and *A. yiselae* sp. nov., strongly sclerotized, protruding from the center of the tegulum, ventrally directed (Figs 2D–E, 3H–J). Female internal genitalia consisting of a membranous posterior receptacle (pr) covering a pair of horizontal sclerotized bars (psb) which leads with the sclerotized bifid duct (mp) on anteromedian receptacle base (arb); also an anteromedian receptacle formed by a base (arb) leading to a large, oval membranous sac-like structure (sac) covered with scattered accessory gland openings (Figs 6B–D, 11E–F).

Updated key for the species of *Aamunops* Galán-Sánchez & Álvarez-Padilla, 2022

1. Males 2
– Females 7

2. Long embolus, equal to or longer than palpal tibia, with a narrow base and a hyaline process reaching the tip (Galán-Sánchez & Álvarez-Padilla 2022: figs 7, 25, 44) 3
– Short embolus, not as long as palpal tibia, with a wide base and a narrow tip that looks like a triangle in lateral view 5

3. Embolus as long as palpal tibia, distal portion bent (Galán-Sánchez & Álvarez-Padilla 2022: figs 26, 44) 4
– Embolus two times as long as palpal tibia, slender, curved (Galán-Sánchez & Álvarez-Padilla 2022: figs 7, 16) ..... ***A. olmeca*** Galán-Sánchez & Álvarez-Padilla, 2022

4. Thick, rounded embolus tip; swollen cymbium (Galán-Sánchez & Álvarez-Padilla 2022: figs 27, 37) ..... ***A. chimpa*** Galán-Sánchez & Álvarez-Padilla, 2022
– Thin, sharpened embolus tip (Galán-Sánchez & Álvarez-Padilla 2022: fig. 55) ..... ***A. misi*** Galán-Sánchez & Álvarez-Padilla, 2022

5. Slender, sinuous embolus, with a curved or straight tip and a hyaline process very thin 6
– Wide, straight embolus, with a hoof-shaped tip and a hyaline process very wide (Figs 2D–E, 5B) ..... ***A. hoof*** sp. nov.

6. Embolus tip straight with small denticles on the tip and a minute hyaline process (Galán-Sánchez & Álvarez-Padilla 2022: figs 62, 68) ..... ***A. noono*** Galán-Sánchez & Álvarez-Padilla, 2022
– Embolus tip curved without denticles on the tip and a longer and fine hyaline process (Figs 3H–J, 5A) ..... ***A. yiselae*** sp. nov.

7. Anteromedian receptacle with a V-shaped sclerotized bifid duct (Galán-Sánchez & Álvarez-Padilla 2022: fig. 11) ..... ***A. olmeca*** Galán-Sánchez & Álvarez-Padilla, 2022
– Anteromedian receptacle with a T-shaped sclerotized bifid duct (Fig. 6D) 8

8. Sclerotized bifid duct with a concave anterior margin (Galán-Sánchez & Álvarez-Padilla 2022: fig. 29) 9
– Sclerotized bifid duct with a convex anterior margin (Fig. 6D) ..... ***A. yiselae*** sp. nov.

9. Sclerotized bifid duct long and thin (Galán-Sánchez & Álvarez-Padilla 2022: figs 29–30) .... ***A. chimpa*** Galán-Sánchez & Álvarez-Padilla, 2022
– Sclerotized bifid duct short and wide (Galán-Sánchez & Álvarez-Padilla 2022: figs 48–49) .... ***A. misi*** Galán-Sánchez & Álvarez-Padilla, 2022

Aamunops hoof sp. nov.
urn:lsid:zoobank.org:act:3C53B565-DE2F-4228-ABC2-FC23D37B0AAA
Figs 2, 5B, 13

Diagnosis

The males of *A. hoof* sp. nov. resemble those of *A. noono* and *A. yiselae* sp. nov. by having a short embolus, shorter than the palpal tibia, but can be distinguished by the wide and straight embolus, with a hoof-shaped tip and a very wide hyaline process (Figs 2D, 5B).

Etymology

The specific name refers to the shape of the embolus tip that resembles a horse hoof.

Type material

Holotype

MEXICO • ♂; Guerrero, Tepecoacuilco de Trujano, Cerro de la Coronilla; 18.01628° N, 99.52875° W; 855 m a.s.l.; Oct. 2009; T. López, C. Quijano and A. Valdez leg.; CNAN-Ar 9727.

Description

Male (holotype)

Carapace orange (Fig. 2C). Chelicerae, palps, endites, labium, sternum and legs light orange; tibia, metatarsi and tarsi lighter. Abdomen pale gray, without dorsal pattern. Anal tubercle and spinnerets lighter than abdomen. Crista short, covering less than half of metatarsi of legs I–II. Total length 3.5. Carapace 1.4 long, 0.9 wide. Sternum 1.3 long, 0.8 wide. Leg measurements: I: 4.0; II: 3.7; III: 2.9; IV: 4.2. Tegulum globose, spherical; embolus short, wide, length hardly reaching middle of palpal tibia length, with hoof-shaped tip, spermatic duct with very wide hyaline process at tip of embolus (Figs 2D, 5B).

Female

Unknown.

Distribution

Known only from the type locality in Mexico (Fig. 13).

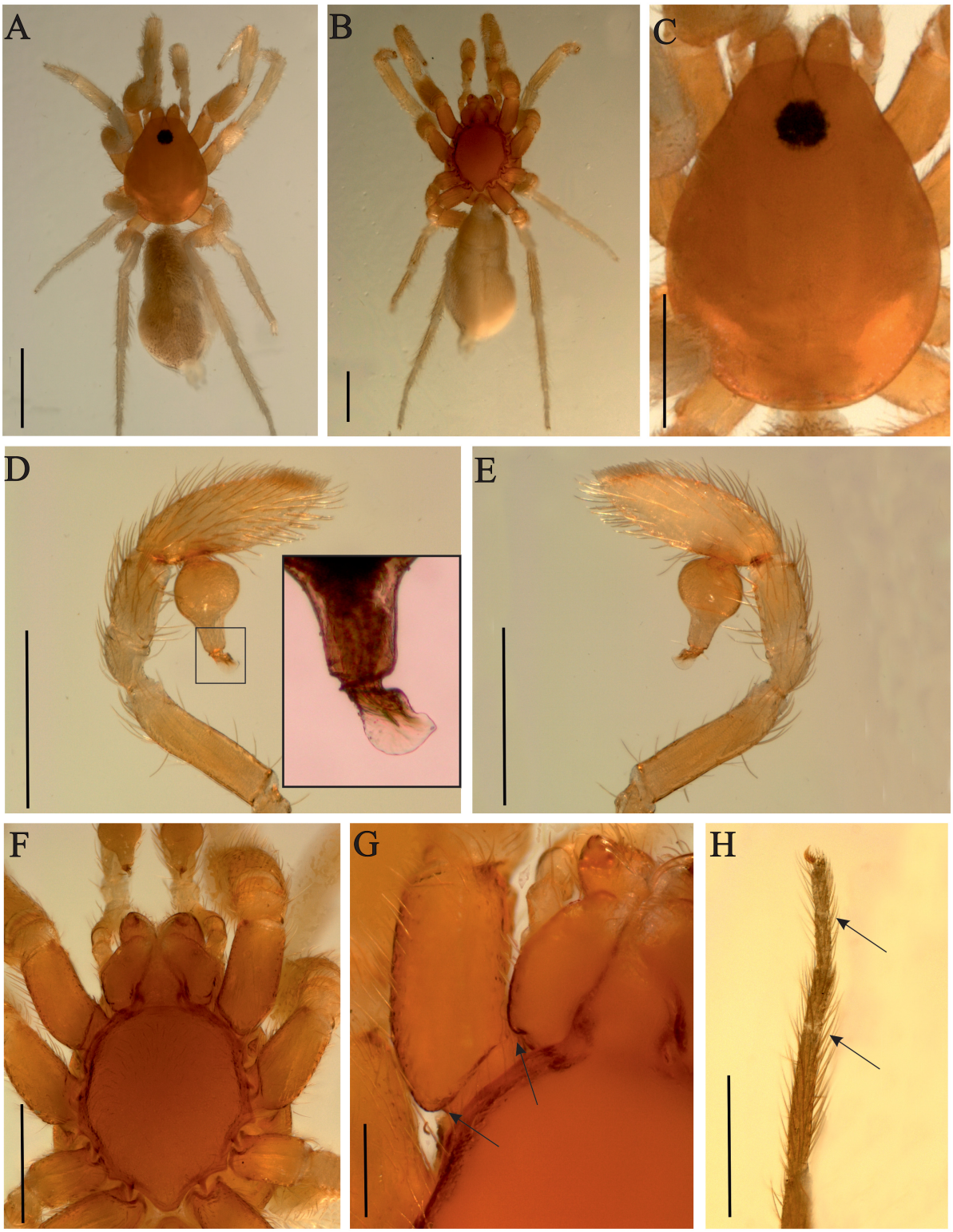

Fig. 2. *Aamunops hoof* sp. nov., holotype, ♂ (CNAN-Ar 9727). **A**. Habitus, dorsal view. **B**. Habitus, ventral view. **C**. Carapace, dorsal view. **D**. Left palp, in square a detail of the embolus tip, prolateral view. **E**. Left palp, retrolateral view. **F**. Sternum and mouth parts, ventral view. **G**. Right coxa I and endite, arrows show the basal posterior projections, ventral view. **H**. Right leg IV, arrows show the adesmatic joints, retrolateral view. Scale bars: A–B = 1 mm; C–F = 0.5 mm; G–H = 0.2 mm.

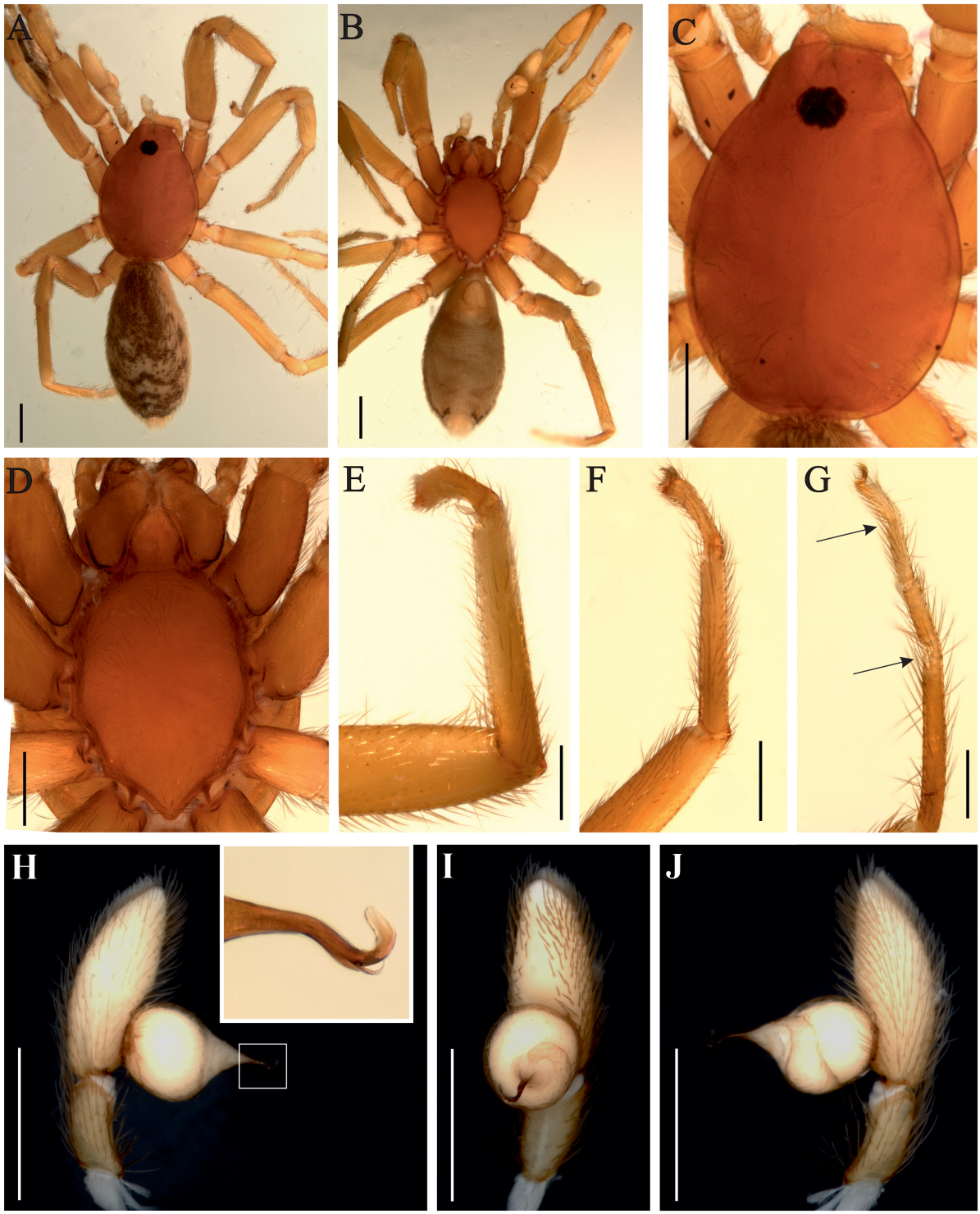

Fig. 3. *Aamunops yiselae* sp. nov., holotype, ♂ (CNAN-Ar 6948). **A**. Habitus, dorsal view. **B**. Habitus, ventral view. **C**. Carapace, dorsal view. **D**. Sternum and mouth parts, ventral view. **E**. Right leg I, prolateral view. **F**. Right leg III, prolateral view. **G**. Right leg IV, prolateral view, arrows show the adesmatic joints. **H**. Left palp, in square a detail of the embolus tip, prolateral view. **I**. Left palp, ventral view. **J**. Left palp, retrolateral view. Scale bars = 0.5 mm.

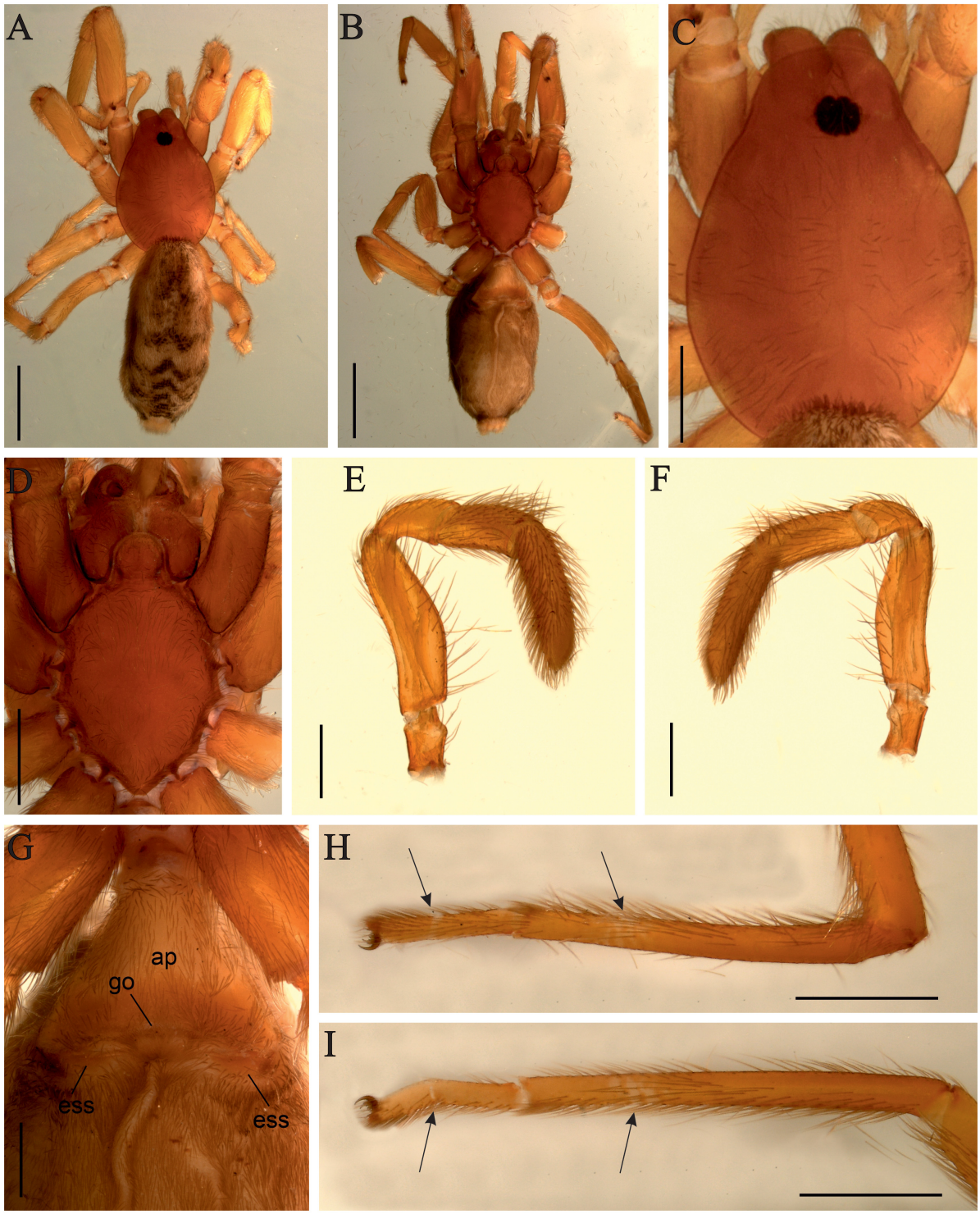

Fig. 4. *Aamunops yiselae* sp. nov., paratype, ♀ (CNAN-Ar 6945). **A**. Habitus, dorsal view. **B**. Habitus, ventral view. **C**. Carapace, dorsal view. **D**. Sternum and mouth parts, ventral view. **E**. Left palp, prolateral view. **F**. Left palp, retrolateral view. **G**. External genital area, ventral view. **H**. Right tarsus and metatarsus IV, prolateral view, arrows show the adesmatic joints. **I**. Left tarsus and metatarsus IV, retrolateral view, arrows show the adesmatic joints. Abbreviations: see Material and methods. Scale bars: A–B = 1 mm; C–G = 0.5 mm; H–I = 0.2 mm.

Aamunops yiselae sp. nov.
urn:lsid:zoobank.org:act:16C669C8-4F61-4D28-B800-E48B669E1C25
Figs 3–4, 5A, 6–13

Diagnosis

The males of *A. yiselae* sp. nov. resemble those of *A. noono* and *A. hoof* sp. nov. by having a short embolus, shorter than the palpal tibia, but can be distinguished by a slender and sinuous embolus tip, without denticles and with a longer and thin hyaline process (Figs 3H, 5A). Females can be distinguished from those of the other species with a T-shaped sclerotized bifid duct on the anteromedian receptacle base by having it with a convex anterior margin (Fig. 6D) (vs concave anterior margin in other species).

Etymology

The specific name is a patronym honoring Yisel Krauß, the sister of the first author.

Type material

Holotype

MEXICO • ♂; Oaxaca, 1 km S San Lorenzo Mixtepec; 16.17493° N, 96.20910° W; 2120 m a.s.l.; 23 Jun. 2006; O. Francke, G. Villegas, H. Montaño, A. Valdez and C. Santibañez leg.; CNAN-Ar 6948.

Paratypes

MEXICO • 2 ♀♀; same collection data as for holotype; CNAN-Ar 6945.

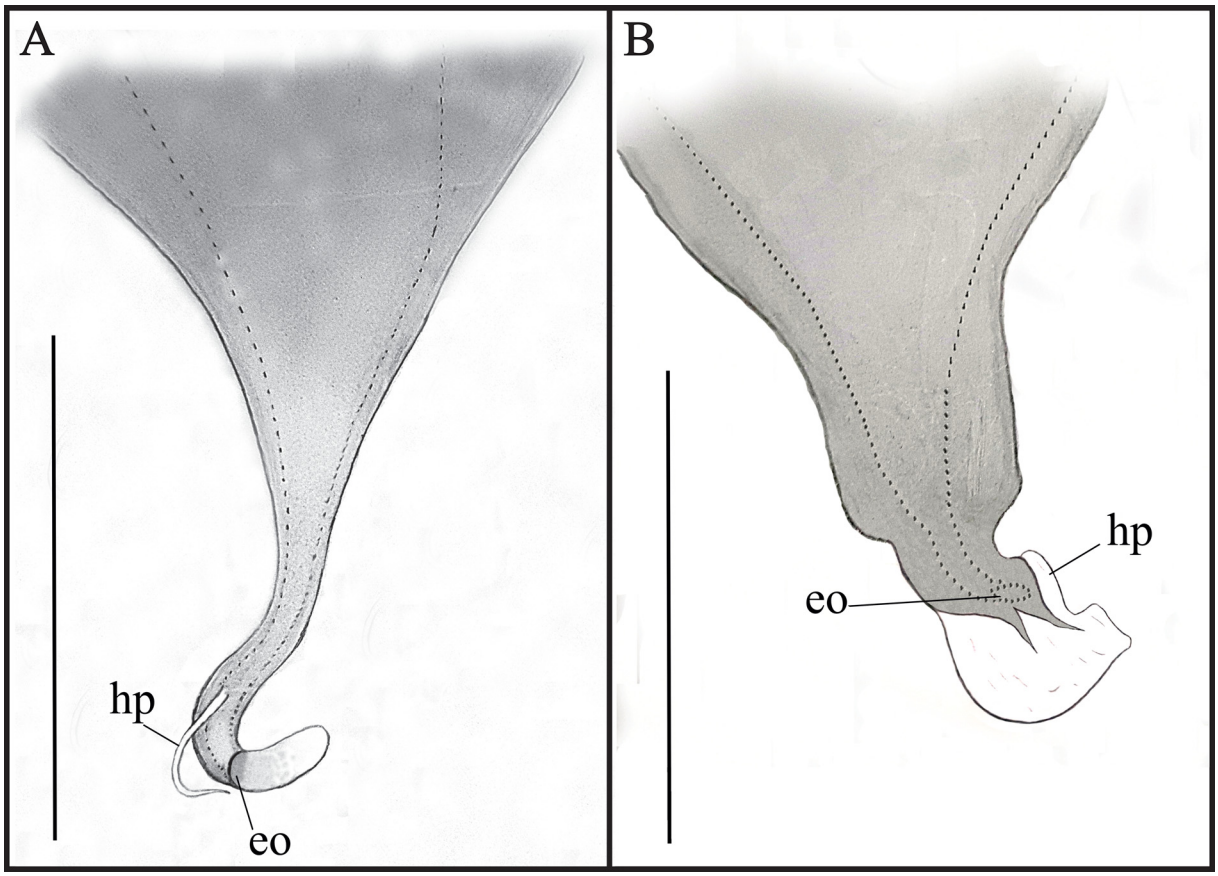

Fig. 5. Drawings of the embolus tip, prolateral view. **A**. *Aamunops yiselae* sp. nov., **B**. *Aamunops hoof* sp. nov. Abbreviations: see Material and methods. Scale bars = 0.1 mm.

Description

Male (holotype)

Carapace orange (Fig. 3C). Chelicerae, palps, endites, labium, sternum and legs light orange; coxae and trochanters lighter. Abdomen pale gray, with dorsal dark gray chevron pattern as in Fig. 3A; ventral part pale gray without stains (Fig. 3B). Anal tubercle and spinnerets lighter than abdomen. Crista short, covering little more than half of metatarsus I, covering less than half of metatarsus II. Total length 3.9. Carapace 1.8 long, 1.3 wide. Sternum 1.6 long, 1.2 wide. Leg measurements: I: 5.3; II: 5.0; III: 4.7; IV:

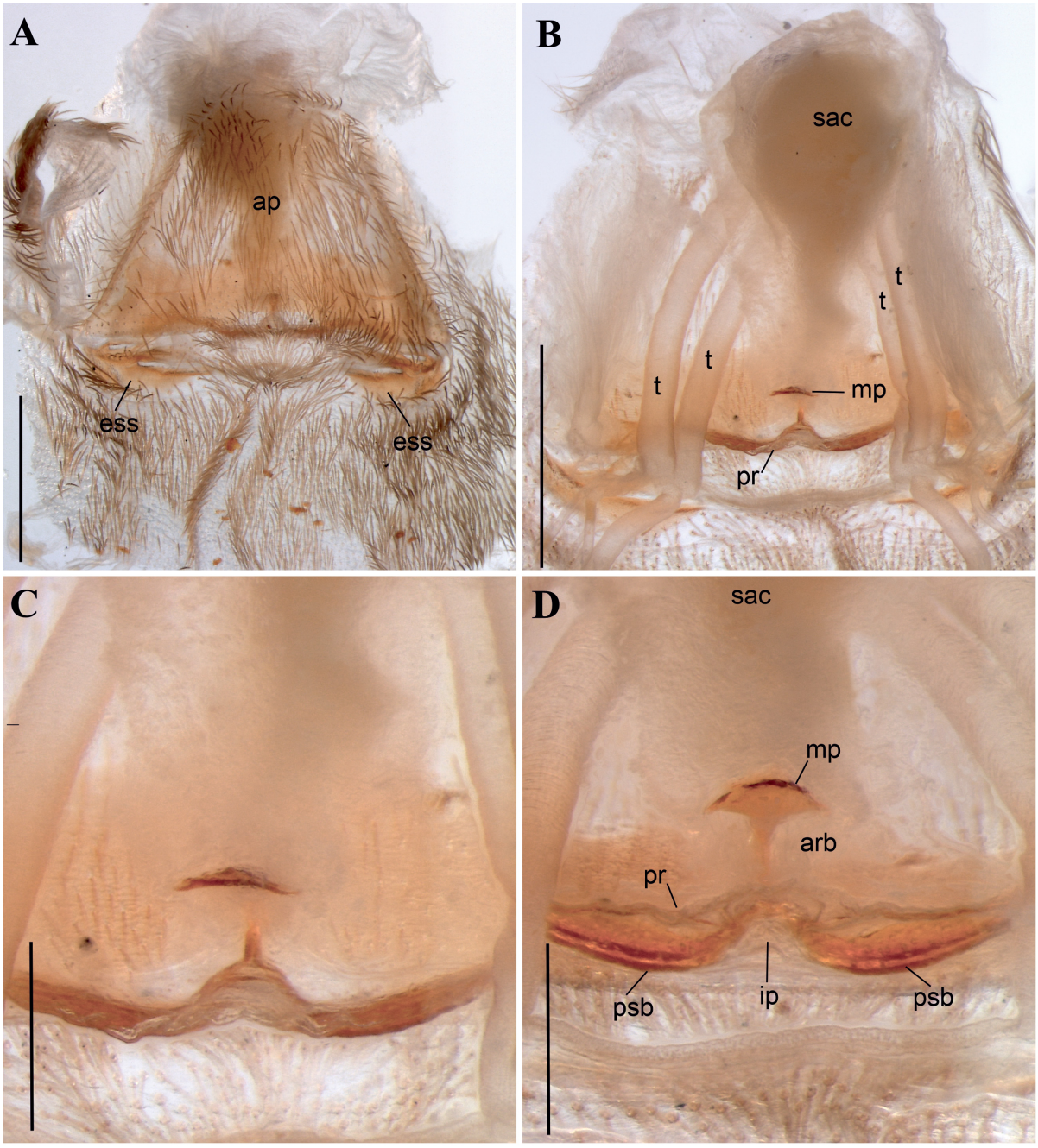

Fig. 6. *Aamunops yiselae* sp. nov., paratype, ♀ (CNAN-Ar 6945). **A**. External genital area, ventral view. **B**. Internal genitalia, dorsal view. **C**. Detail of anteromedian receptaculum base, dorsal view. **D**. Same, posterior view. Abbreviations: see Material and methods. Scale bars: A–B = 0.5 mm, C–D = 0.2 mm.

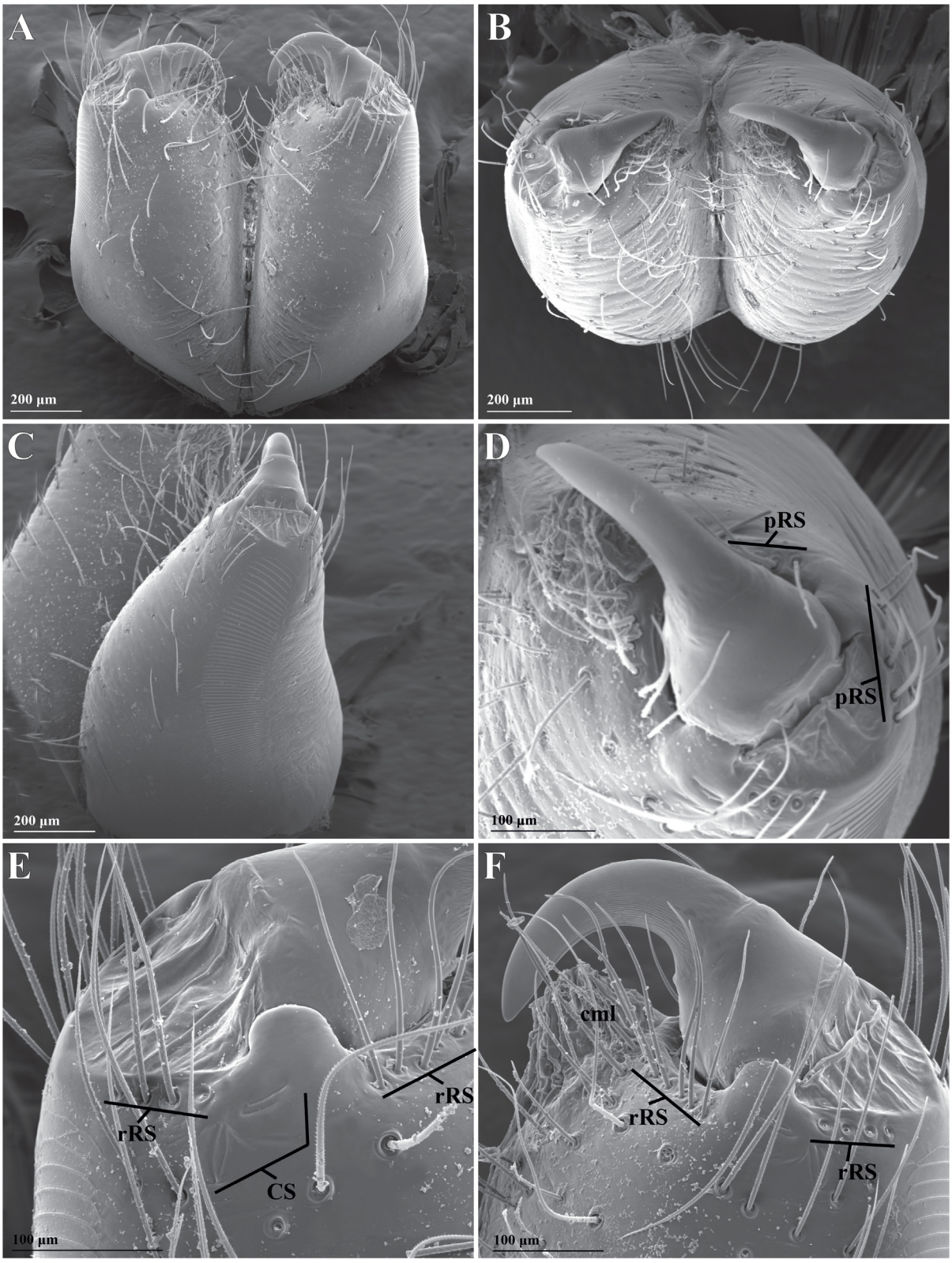

Fig. 7. *Aamunops yiselae* sp. nov., paratype, ♀ (CNAN-Ar 6945), chelicerae. **A**. Anterior view. **B**. Ventral view. **C**. Ectal side showing stridulatory ridges. **D**. Right fang, ventral view. **E**. Detail of left fang base, anterior view. **F**. Detail of right fang base, anterior view. Abbreviations: see Material and methods.

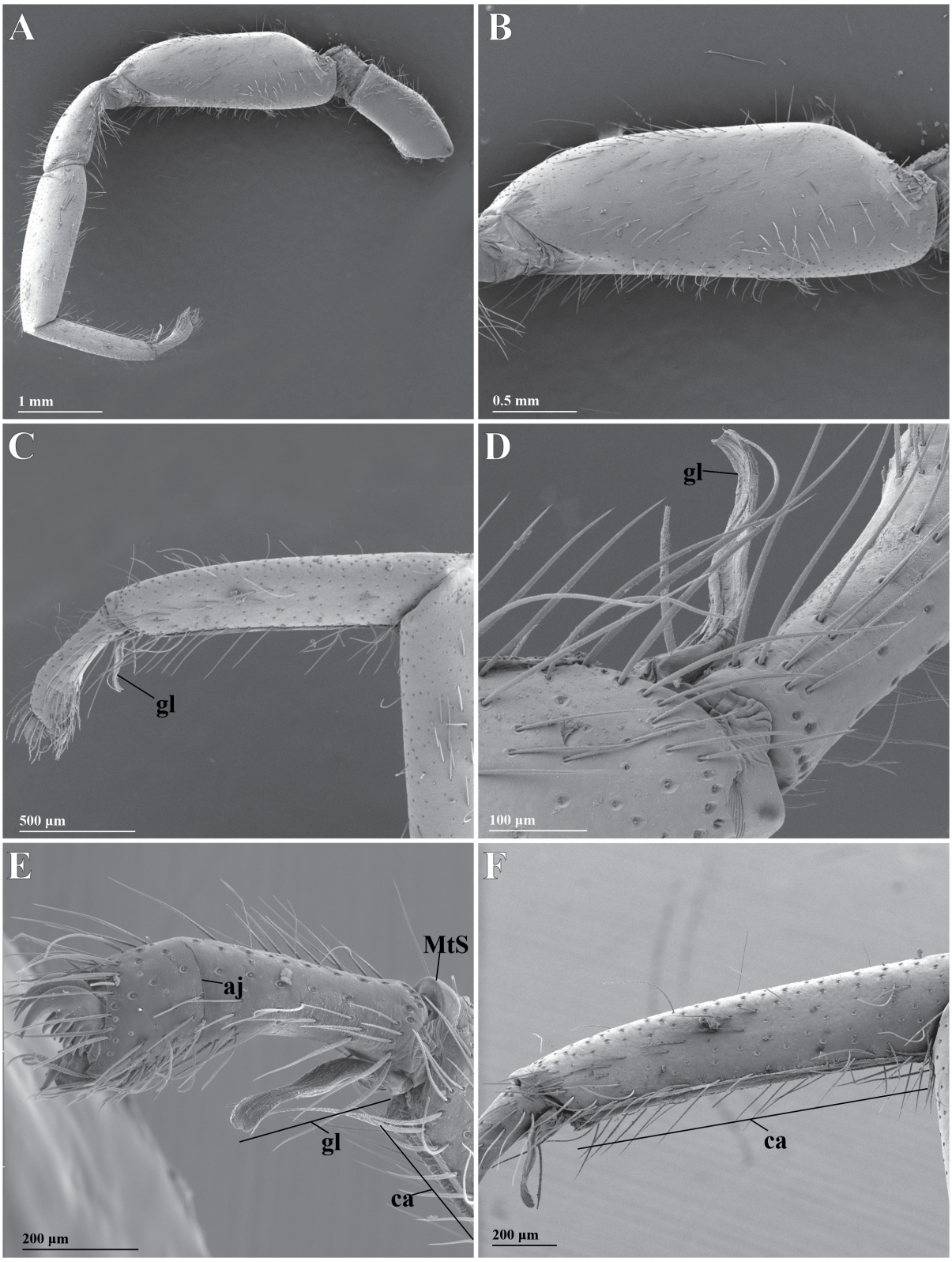

Fig. 8. *Aamunops yiselae* sp. nov., paratype, ♀ (CNAN-Ar 6945), left leg I, retrolateral view. **A**. Full leg. **B**. Femur. **C**. Metatarsus and tarsus. **D**. Gladius on joint of metatarsus and tarsus. **E**. Tarsus. **F**. Metatarsus. Abbreviations: see Material and methods.

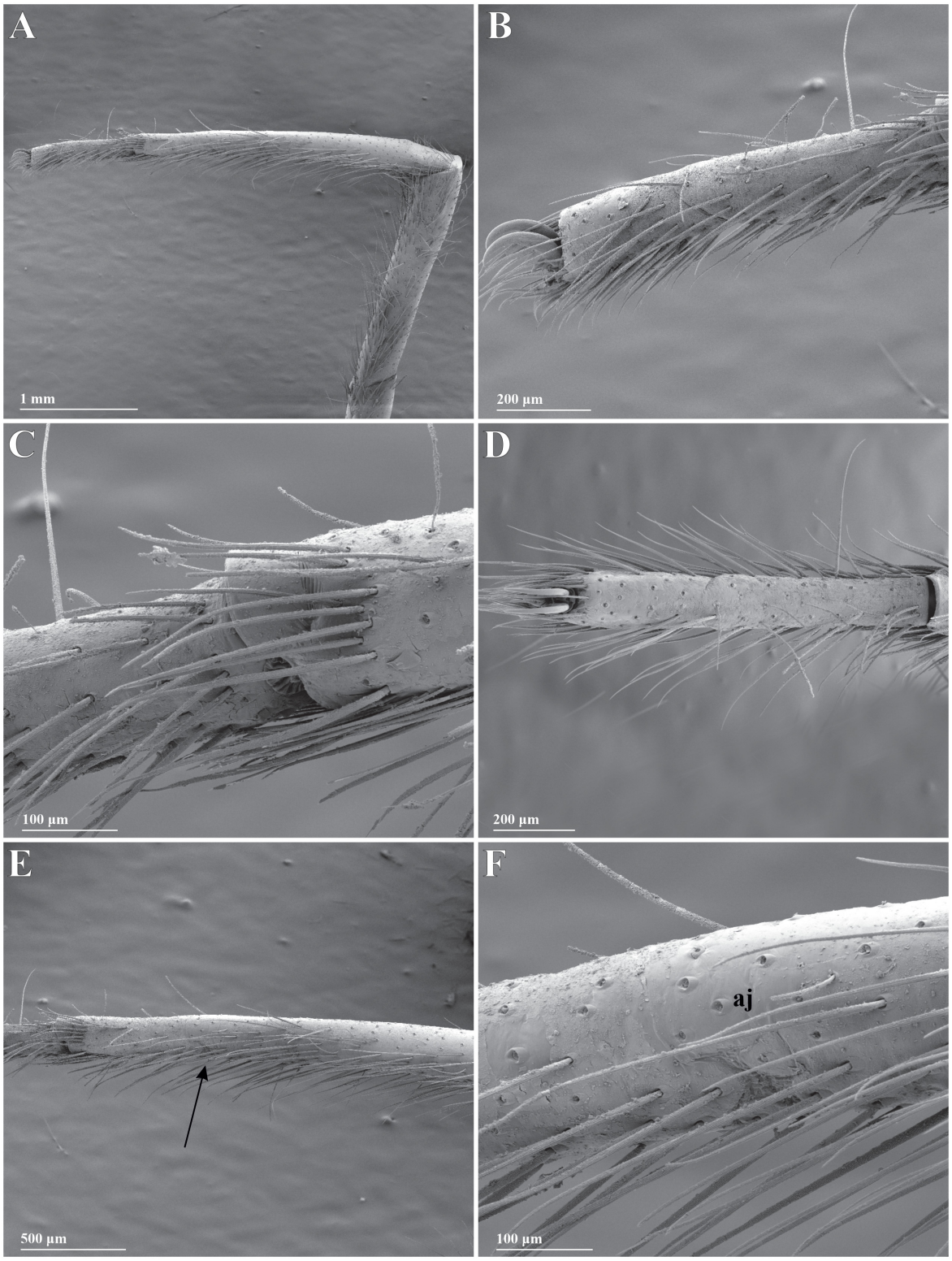

Fig. 9. *Aamunops yiselae* sp. nov., paratype, ♀ (CNAN-Ar 6945), left leg IV. **A**. femur, metatarsus and tarsus, prolateral view. **B**. Tarsus, prolateral view. **C**. Detail of joint metatarsus and tarsus, prolateral oblique view. **D**. Tarsus, dorsal view. **E**. Metatarsus, arrow points adesmatic joint, prolateral oblique view. **F**. Detail of adesmatic joint on metatarsus, prolateral oblique view. Abbreviations: see Material and methods.

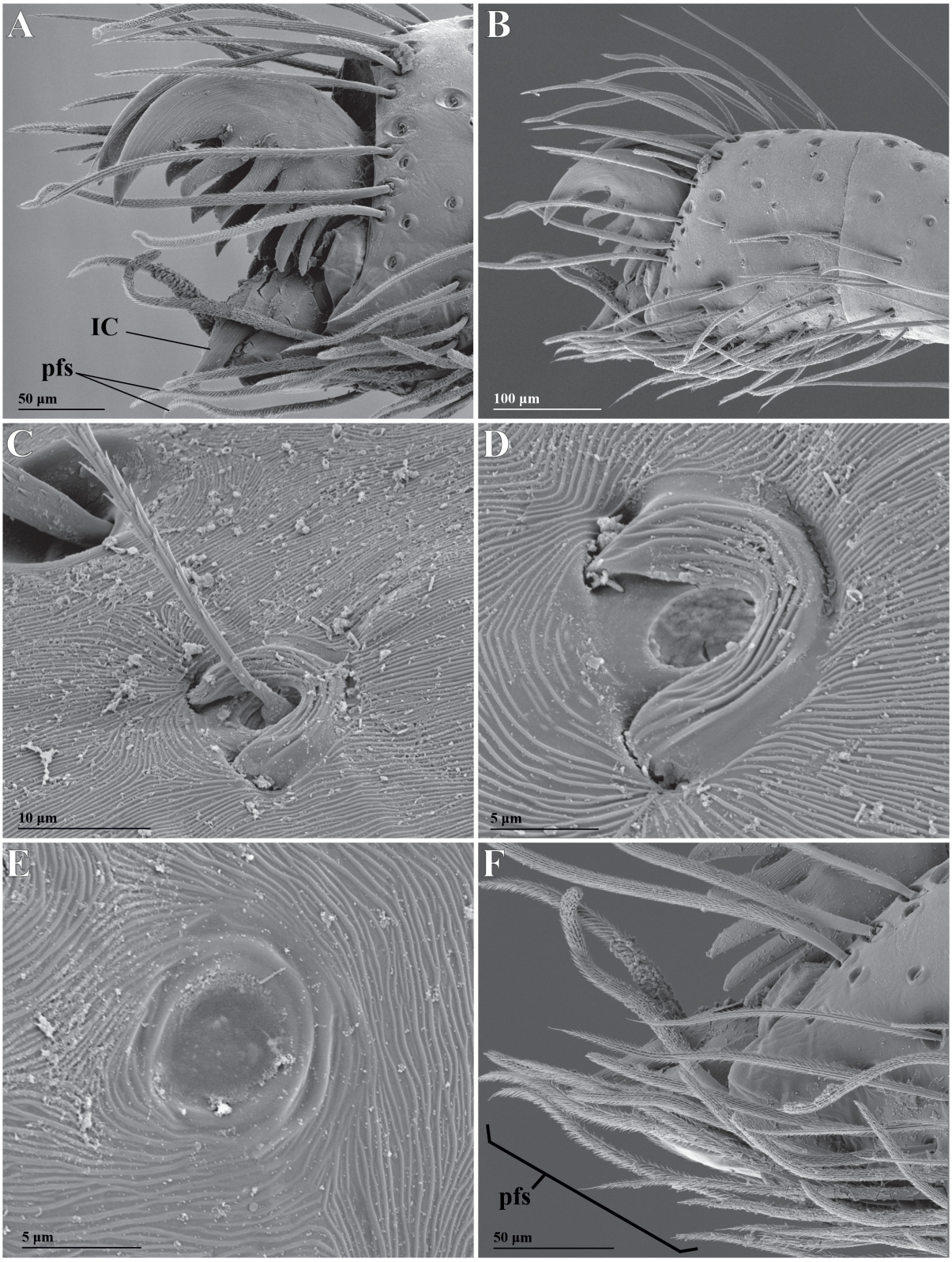

Fig. 10. *Aamunops yiselae* sp. nov., paratype, ♀ (CNAN-Ar 6945). **A**. Left pretarsus I, retrolateral view. **B**. Left tarsus I, retrolateral view. **C**. Trichobothrium on left metatarsus I, dorsal oblique view. **D**. Detail trichobothrium base on left tarsus I, dorsal oblique view. **E**. Tarsal organ, dorsal view. **F**. Ventral frictional setae on left pretarsus I, retrolateral oblique view. Abbreviations: see Material and methods.

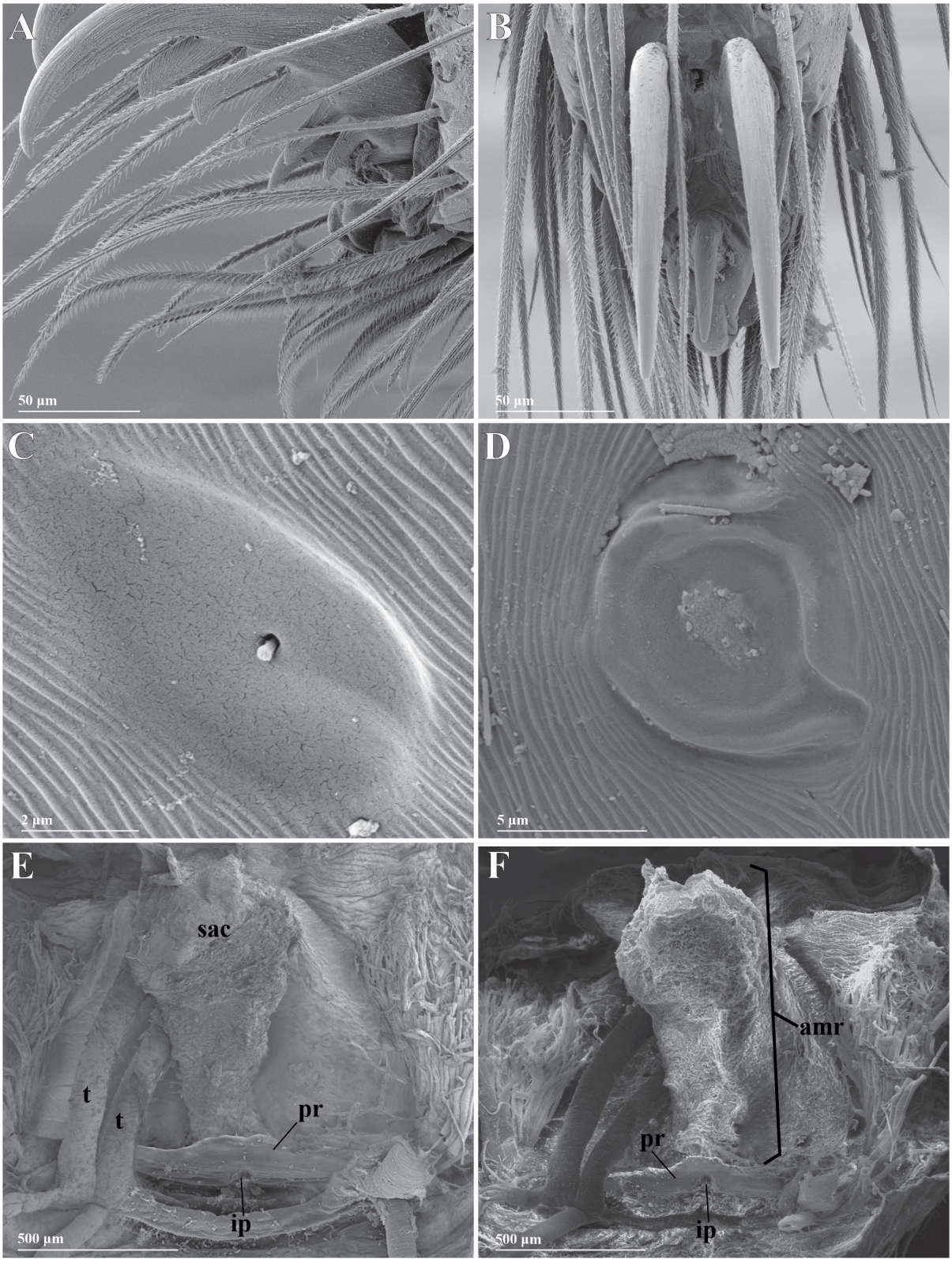

Fig. 11. *Aamunops yiselae* sp. nov., paratype, ♀ (CNAN-Ar 6945). **A**. Left pretarsus IV, prolateral view. **B**. Left pretarsus IV, anterior view. **C**. Presumed slit sensilla on left tarsus IV, dorsal view. **D**. Tarsal organ, dorsal view. **E**. Internal genitalia, ventral view. **F**. Same, posterior view. Abbreviations: see Material and methods.

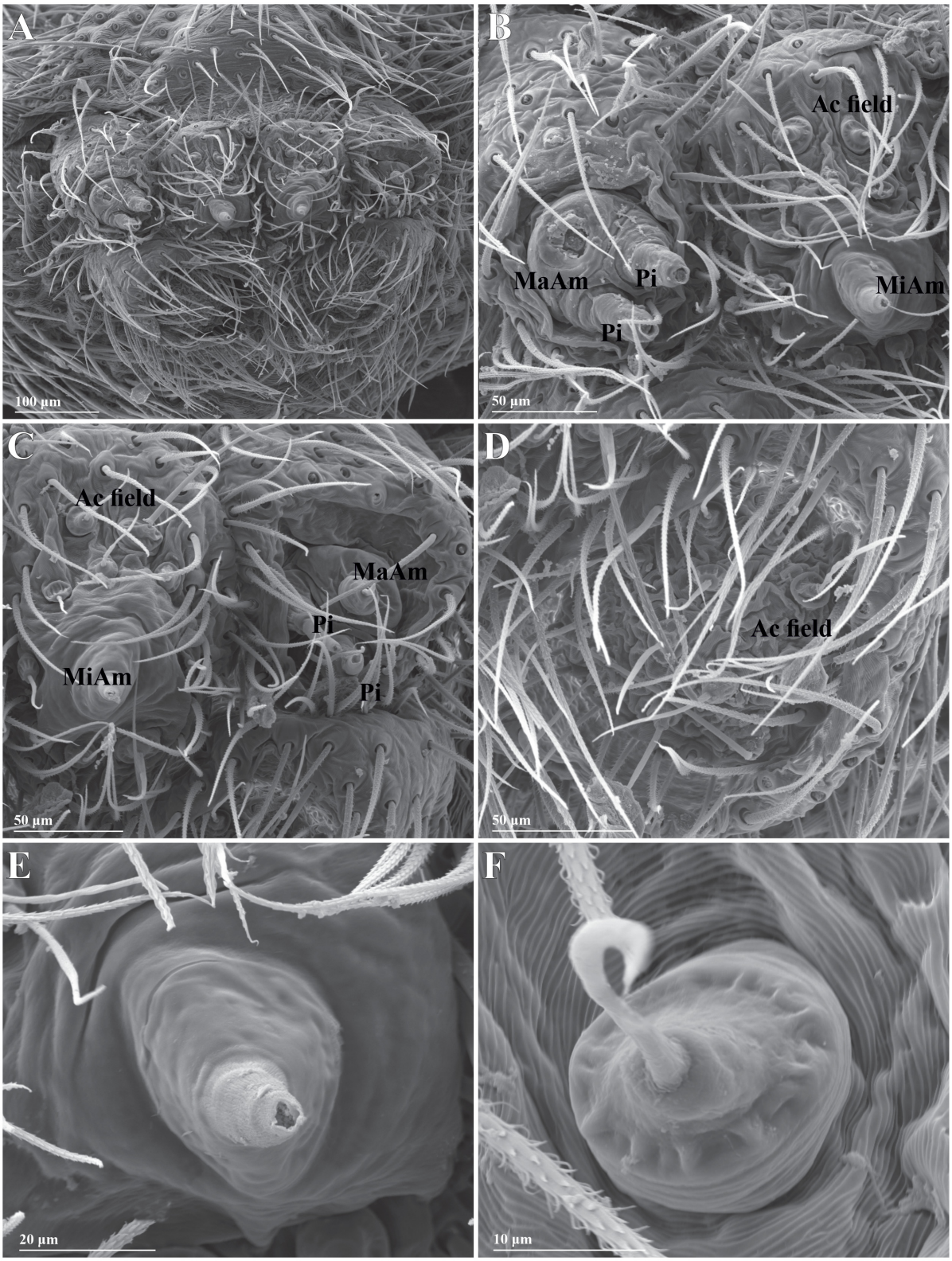

Fig. 12. *Aamunops yiselae* sp. nov., paratype, ♀ (CNAN-Ar 6945), spinnerets, posterior view. **A**. Spinning field. **B**. Left ALS and PMS. **C**. Right ALS and PMS. **D**. Right PMS. **E**. Detail of presumed minor ampullated gland spigot on PMS. **F**. Detail of aciniform gland spigot on AMS. Abbreviations: see Material and methods.

5.5. Tegulum globose, spherical; embolus short, length not reaching palpal tibia length, with wide base and narrow tip that looks like triangle in lateral view, with slender and sinuous embolus tip, without denticles and with long and thin hyaline process (Figs 3H, 5A).

Female (paratype)

Carapace, chelicerae, palps, endites, labium, sternum, coxae, legs, abdomen, anal tubercle and spinnerets as in male (Fig. 4A–D). Crista covering all ventral part of metatarsi. Total length 4.2. Carapace 2.0 long, 1.5 wide. Sternum 1.9 long, 1.5 wide. Leg measurements: I: 5.4; II: 5.2; III: 4.9; IV: 5.6. External genital area with strongly sclerotized ess (Fig. 6A). Internal genitalia with T-shaped sclerotized bifid duct on anteromedian receptacle base and convex anterior margin (Fig. 6D); sac-like membranous structure long and wide (Figs 6B, 11E–F); membranous posterior receptacle covering pair of horizontal sclerotized bars communicating with sclerotized bifid duct on anteromedian receptacle base (Figs 6D, 11E–F).

Distribution

Known only from the type locality in Mexico (Fig. 13).

Discussion

Relationships among the genera of Nopinae

All nopine genera, except for *Orthonops*, are recovered as monophyletic (jackknifing = 57%–98%; BS = 1–5). *Orthonops confuso* is one of the species whose taxonomic position is in doubt. Although its palpal morphology resembles that described for the genus (Platnick 1995), this species is unique among *Orthonops* in having a prolateral tibial brush (18[1]) and lacking a crista (12[0]) (Galán-Sánchez & Álvarez-Padilla 2022). Such characteristics, outside the diagnosis of the genus, could explain why *Orthonops* is not recovered as a monophyletic group (Fig. 1). As presently composed, *Orthonops* is a poorly understood complex of species that may even include undescribed genera and deserves further attention from taxonomists.

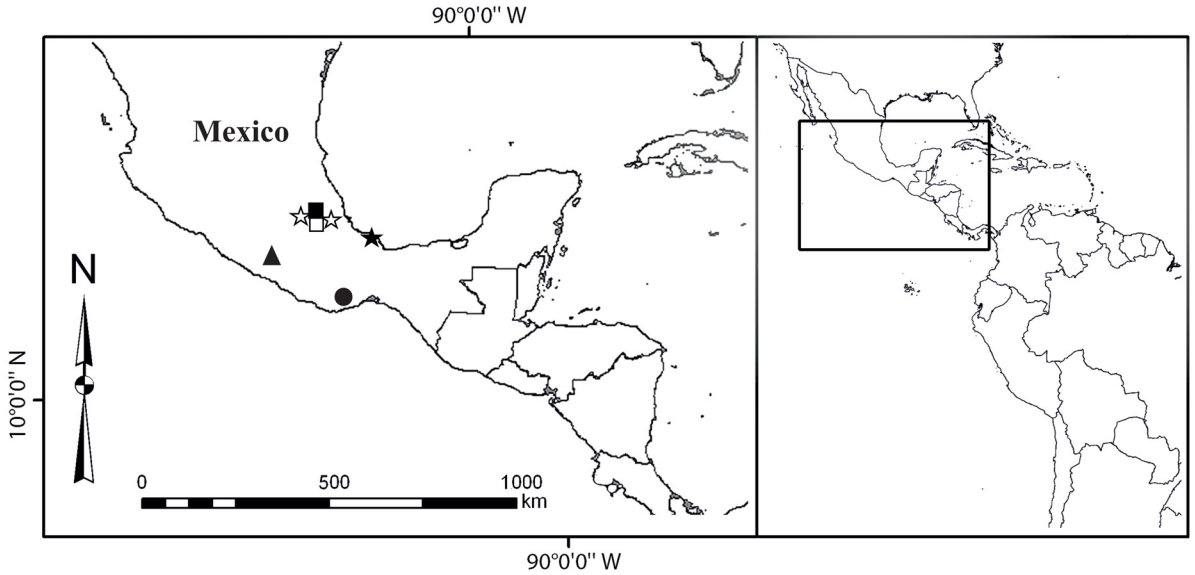

Fig. 13. Distribution map of species of *Aamunops* Galán-Sánchez & Álvarez-Padilla, 2022. *Aamunops chimpa* Galán-Sánchez & Álvarez-Padilla (black square), *A. hoof* sp. nov. (triangle), *A. misi* Galán-Sánchez & Álvarez-Padilla (white stars), *A. noono* Galán-Sánchez & Álvarez-Padilla (white square), *A. yiselae* sp. nov. (circle) and *A. olmeca* Galán-Sánchez & Álvarez-Padilla (black star).

By contrast, the other two species with doubtful taxonomic positions (*Cubanops luquillo* and *Tarsonops irataylori*) were confirmed with high branch support values within each genus they were described in (jackknifing = 85%, BS = 2 for *Cubanops* and jackknifing = 89%, BS = 5 for *Tarsonops*). *Cubanops luquillo* shares several traits with other species of the genus: widened labium, endites medially narrowed, carapace sub-circular and a bisegmented metatarsi IV. However, both the carapace and the abdomen of *C. luquillo* are uniformly colored, lacking the distinct pattern characteristic of all other congeners. Another interesting feature of this species is the presence of a short crista, occupying only about half the length of the metatarsus, while in other species of *Cubanops* the crista occupies the entire metatarsus. According to Sánchez-Ruiz & Brescovit (2018), the crista, gladius and arolium are membranous structures that seem to appear and disappear with more ease than other structures during evolution of caponiids. Given the present results, these discrepancies must be interpreted as autapomorphic. Significantly, *C. luquillo* represents the first and only record of *Cubanops* from the island of Puerto Rico. *Tarsonops irataylori* was also confirmed within the genus in which it was described, but this species only differs from the rest of the congeners by the absence of the crista. Since the monophyly of *Tarsonops* (including *T. irataylori*) was recovered with high branch support, the lack of crista in this species must be considered as a secondary loss.

Basal species in Nopinae

Contrary to the results obtained by Sánchez-Ruiz & Brescovit (2018) and Galán-Sánchez & Álvarez-Padilla (2022), *Nopsides ceralbonus* was recovered as the most basal species of the nopines. Platnick & Lise (2007) supposed that representatives of *Nyetnops* should be regarded as such, due to the absence of the membranous structures in the legs (crista and gladius). Even in the topologies proposed by Sánchez-Ruiz & Brescovit (2018) and Galán-Sánchez & Álvarez-Padilla (2022), *Nyetnops* is recovered as the most basal member of nopines. This hypothesis became disputable when the absence of crista and gladius was observed in species belonging to genera whose members generally present it or with the discovery that these structures could vary even at intraspecific level. Also, the recent description of *Nopsma*, whose representatives do not have a crista, made it more evident that these structures are notably plastic. Our results point to a scenario in which the crista appeared early, in a clade composed by all nopine lineages but *Nopsides*, with subsequent, independent losses in *Orthonops confuso* and in the clade *Nopsma*+*Nyetnops*. In effect, it makes much more sense then that the basal species of all nopines is precisely *Nopsides*, a monotypic genus harboring the only four-eyed nopine species, clearly a plesiomorphic character (Sánchez-Ruiz & Brescovit 2018). Most caponiids lack eyes, but *Caponia* and *Calponia*, apparently the oldest members of the family, retain eight eyes (Platnick 1993).

Acknowledgments

We thank all curators and collection managers listed in Material and methods for providing loans and allowing us to study the specimens. Antonio Galán-Sánchez provided very useful information about *Aamunops*, and Hilton Túlio Costi helped to obtain SEM micrographs at Museu Paraense Emilio Goeldi. We thank the section editor Rudy Jocqué and the two reviewers, Fernando Álvarez-Padilla and a anonymous reviewer, for their useful suggestions on the manuscript. This paper was supported by the Programa de Capacitação Institucional (MCTI/MPEG/CNPq process 444338/2018-7), CNPq grant 300856/2022-9 to ASR, and by CNPq PQ grant #307165/2022-1 to ABB.

References

Brescovit A.D. & Sánchez-Ruiz A. 2016. Descriptions of two new genera of the spider family Caponiidae (Arachnida, Araneae) and an update of *Tisentnops* and *Taintnops* from Brazil and Chile. *ZooKeys* 622: 47–84. https://doi.org/10.3897/zookeys.622.8682

Galán-Sánchez M.A. & Álvarez-Padilla F. 2022. A new genus of caponiid spiders with its phylogenetic placement within Nopinae and the description of a new species of *Orthonops* Chamberlin, 1924 from Eastern Mexico (Araneae: Synspermiata, Caponiidae). *Zootaxa* 5128 (4): 547–573. https://doi.org/10.11646/zootaxa.5128.4.5

Goloboff P.A, Farris J.S. & Nixon K.C. 2008. TNT, a free program for phylogenetic analysis. *Cladistics* 24: 774–786. https://doi.org/10.1111/j.1096-0031.2008.00217.x

Nixon K.C. 2002. WinClada. Version 1.00.08. Published by the author, Ithaca, New York.

Platnick N.I. 1993. A new genus of the spider family Caponiidae (Araneae, Haplogynae) from California. *American Museum Novitates* 3063: 1–8. Available from http://hdl.handle.net/2246/5024 [accessed 26 Feb. 2024].

Platnick N.I. 1995. A revision of the spider genus *Orthonops* (Araneae, Caponiidae). *American Museum Novitates* 3150: 1–18. Available from https://www.biodiversitylibrary.org/page/62188370 [accessed 26 Feb. 2024].

Platnick N.I. & Lise A.A. 2007. On *Nyetnops*, a new genus of the spider subfamily Nopinae (Araneae, Caponiidae) from Brazil. *American Museum Novitates* 3595: 1–9. https://doi.org/10.1206/0003-0082(2007)3595[1:ONANGO]2.0.CO;2

Sánchez-Ruiz A. & Bonaldo A.B. 2023. Strange new spiders: On *Roddenberryus*, a new and unusual caponiid genus (Araneae, Caponiidae). *European Journal of Taxonomy* 891: 1–25. https://doi.org/10.5852/ejt.2023.891.2263

Sánchez-Ruiz A. & Brescovit A.D. 2015. On the taxonomic placement of the Cuban spider *Nops ariguanabo* Alayón and the description of a new Mexican *Tarsonops* (Araneae, Caponiidae). *Zootaxa* 3914 (2): 131–143. https://doi.org/10.11646/zootaxa.3914.2.3

Sánchez-Ruiz A. & Brescovit A.D. 2017. A new genus with seven species of the Subfamily Nopinae (Araneae, Caponiidae) from the Neotropical region. *Zootaxa* 4291 (1): 117–143. https://doi.org/10.11646/zootaxa.4291.1.7

Sánchez-Ruiz A. & Brescovit A.D. 2018. A revision of the Neotropical spider genus *Nops* MacLeay (Araneae: Caponiidae) with the first phylogenetic hypothesis for the Nopinae genera. *Zootaxa* 4427 (1): 1–121. https://doi.org/10.11646/zootaxa.4427.1.1

Sánchez-Ruiz A., Platnick N.I. & Dupérré N. 2010. A new genus of the spider family Caponiidae (Araneae, Haplogynae) from the West Indies. *American Museum Novitates* 3705: 1–44. https://doi.org/10.1206/3705.2

Sánchez-Ruiz A., Brescovit A.D. & Alayón G. 2015. Four new caponiids species (Araneae, Caponiidae) from the West Indies and redescription of *Nops blandus* (Bryant). *Zootaxa* 3972 (1): 43–64. https://doi.org/10.11646/zootaxa.3972.1.3

Manuscript received: 13 February 2023
Manuscript accepted: 23 November 2023
Published on: 3 April 2024
Topic editor: Magalie Castelin
Section editor: Rudy C.A.M. Jocqué
Desk editor: Radka Rosenbaumová

Supplementary files

Supp. file 1. Data matrix for cladistic analysis.
https://doi.org/10.5852/ejt.2024.930.2493.11133

Supp. file 2. Terminal taxa scored for the cladistic analysis, with origin and depository.
https://doi.org/10.5852/ejt.2024.930.2493.11135

Supp. file 3. Characters scored for cladistic analysis.
https://doi.org/10.5852/ejt.2024.930.2493.11137